Journal of Solar Energy Research (JSER)

Journal homepage: www.jser.ut.ac.ir

Analysis and Design of a New DC-DC Converter for DC Smart Grid

Homa Zarei Zohdi[a] , Mohammad Sarvi[b,*]

[a] *Electrical Engineering Department, Imam Khomeini International University, Qazvin, Iran.*
[b] *Electrical Engineering Department, Iran University of Science and Technology, Tehran, Iran.*

ARTICLE INFO

Article Type:

Research Article

Received:30.03.2023
Accepted:06.06.2023

Keywords:
DC-DC Converter
DC Smart Grid
Battery Charging
MPPT

A B S T R A C T

Due to the increasing penetration of distributed generation systems, the desire to use DC smart grids has increased. DC smart grids are preferred to AC grids because these networks are more compatible with renewable sources that generate DC electricity. This paper presents the design of a new three-port isolated DC-DC converter for photovoltaic (PV)-battery application in the DC smart grid. In the proposed converter, by combining the required converters for PV and battery, the number of required converters has been reduced so that the function of charging/discharging the battery, as well as tracking the maximum power point of solar panels, can be done with the proposed converter. As a result, the number of required parts and the cost of the system are reduced and the efficiency of the converter increases. Finally, the converter's performance has been evaluated with the help of analysis and simulation, and the obtained results indicate the proper performance of the proposed converter.

1. Introduction

The use of fossil fuels has increased significantly in the last decade, which has led to environmental pollution and increased system costs [1]. These problems attract researchers to work on distributed generation sources such as photovoltaics (PV) and wind turbines [2]. Smart DC grids have many advantages, one of the most important of which is the use of renewable sources, which are DC sources by nature, and therefore require only one power conversion step to connect to the DC grid [3]. Also, many loads require a DC source [4]. DC-DC converters are used for DC grids and can provide functions such as power flow control, grid voltage regulation, and coupling between two DC systems [5].

*Corresponding Author Email: msarvi@iust.ac.ir

Cite this article: Zarei Zohdi, H., & Sarvi, M. (2023). Analysis and Design of a New DC-DC Converter for DC Smart Grid. Journal of Solar Energy Research, 8(2), 1547-1558.

DOI: 10.22059/jser.2023.357223.1290 DOR: 20.1001.1.25883097.2023.8.2.15.3

Considering that the production of energy from renewable sources depends on environmental conditions, in a smart grid, the existence of an energy storage system such as a battery is necessary to create energy stability [6]. A bidirectional DC-DC converter is used to operate the energy storage system, which transfers energy from the renewable source and the battery bidirectionally [7]. Cascaded DC-DC converters are one of the most common converters for integrating energy storage systems into the power grid [8]. Conventional boost converters are unsuitable for high-power applications [9]. Due to some drawbacks of the diode reverse recovery problem, the pressure of high voltages on the switches reduces the efficiency [10]. Xiaofeng Zhang et al. [11] have used a cascaded buck-boost converter in the system. Lee and Yun. [12] have introduced a new buck-boost converter. Zhu et al. [13] have presented an asymmetric converter with two active bridge rectifiers. Revathi and Prabhakar. [14] proposed a non-isolated high-power DC-DC converter powered by a solar panel for use in a DC microgrid, but the number of elements used in the proposed converter is a lot. Rosas-Caro et al. [15] have discussed the second order boost converter with voltage factor, and the presented converter has a flexible structure. Maroti et al. [16] proposed a new structure of SEPIC converter for renewable energy applications, which used hard switching in the converter and reduced the system's efficiency. Mastromauro et al. [17] have used a modular multilevel cascaded converter for a DC bus. Faraji et al. [18] have presented a new bidirectional multiport converter with soft switching for battery and supercapacitor integration in a DC network. Mukherjee et al. [19] have described the performance of a dual active bridge (DAB) converter in PV systems. In solar systems, maximum power point tracking (MPPT) algorithms use to improve system performance [20]. There are many techniques for MPPT in solar systems [21]. Nanshikar and Desai. [22] have used the P&O algorithm for MPPT solar panels in the system. Sarvi and Azadian. [23] have divided the MPPT algorithms by reviewing the articles and introducing the appropriate methods. Masoum and Sarvi. [24] have presented the MPPT algorithm based on the voltage and current of solar arrays under varying temperature and radiation conditions. Bento and Silva. [25] have presented a unidirectional converter that consists of a lot number of switches and inductors to obtain multiple outputs, as a result, the overall efficiency of the system is limited.

According to the investigations, the number of circuit parts effectively improves the efficiency of converters. In this paper, a three-port isolated DC-DC converter is proposed, which has fewer parts and more capabilities than other converters that have been reviewed in the research background. Hence, the converter is more efficient and affordable. The proposed converter offers the ability to connect to photovoltaic panels and charge/discharge the battery for DC smart grid applications. This converter is used to meet the demand of output DC load, which can be DC power supply for homes, electric vehicles and DC microgrids, and battery charging. The overall architecture of the DC smart grid system with PV, battery, and proposed converter is shown in Figure 1.

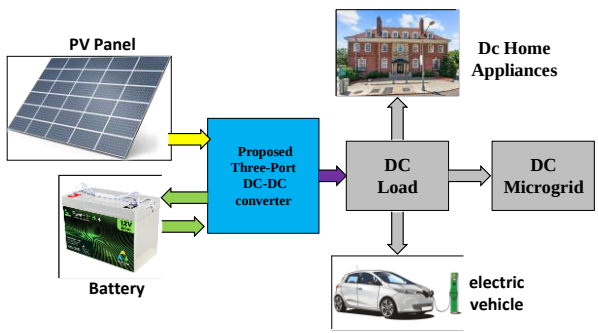

Figure 1. The general architecture of the studied DC smart grid system.

The structure of the continuation of the paper is presented as follows. In Section 2, the topology of the proposed converter and its performance details are prepared. Section 3 is the design considerations. In section 4, the simulation and its results are reviewed. In Section 5, the performance of the converter is compared. In Section 6, conclusions are presented.

2. Description of proposed converter topology and principles of operation

The converter topology is shown in Figure 2. The proposed converter has two input terminals and one output terminal, the first terminal is connected to the solar panel, and the second terminal is connected to the lithium-ion battery. The transformer used in the converter is a step-up type. The primary part is the low voltage side converter (LVS), and the second part is the high voltage side converter (HVS). The LVS side of the converter includes inductors L_1, L_2, and L_3, six switches (MOSFET with N channel) with snubber capacitor C_p, capacitor C_1, and transformer primary winding. The HVS side of the converter

consists of a secondary coil and a diode bridge with D_1-D_4 diodes, and a Cs capacitor filter. A resistive load has been used to simulate the network part in the output of the circuit.

The converter has four general operating modes, each of which is divided into modes, and the modes of each are described. As shown in Figure 3, there are four working modes for the converter.

Mode 1: In mode 1, the photovoltaic panel produces power, and the solar panel is in MPPT tracking mode. Also, in this case, the battery charge is sufficient, and it is discharged. As briefly described in Table 1, mode 1 can be divided into 4 states. The circuit in each of the operating modes is shown in Figure 4. Some of the waveforms of the converter in mode 1 are shown in Figure 5. Since the gate pulses of S_1 and S_2 have a phase difference of 180 degrees, the battery current ripple is almost reduced. The circuit equations, in this case, are extracted as follows [25]:

$$V_1 = V_{bat} + V_{pv} \tag{1}$$

$$V_{out} = V_{cs} \tag{2}$$

$$\frac{V_1}{n} = V_{cs} \tag{3}$$

$$L_3 \frac{di}{dt} = V_{bat} \tag{4}$$

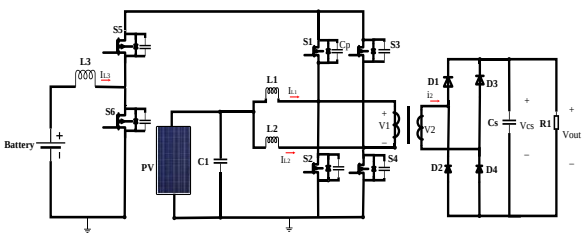

Figure 2. Proposed converter topology.

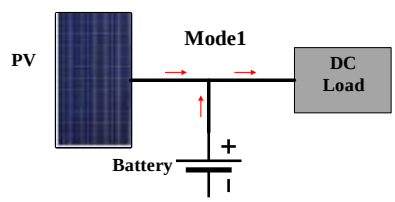

(a)

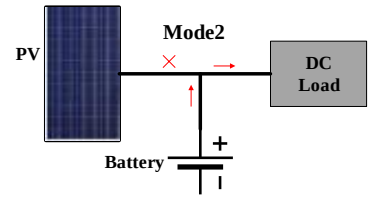

(b)

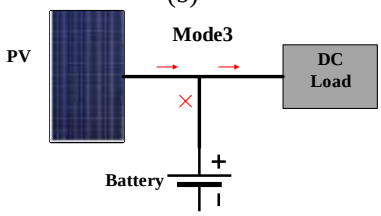

(c)

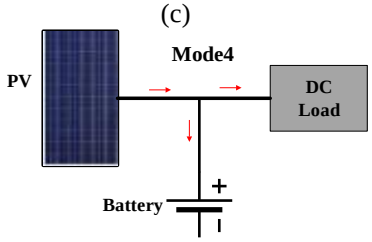

(d)

Figure 3. Four modes of the converter. (a) mode 1, (b) mode 2, (c) mode 3, (d) mode 4.

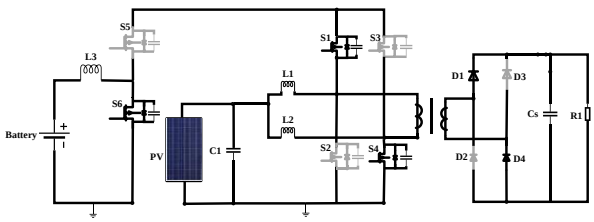

(a)

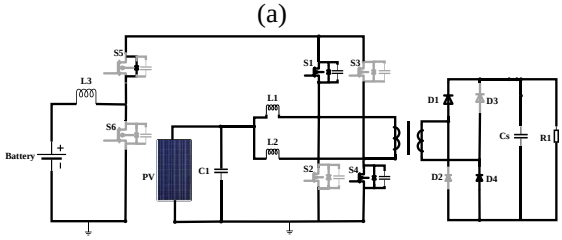

(b)

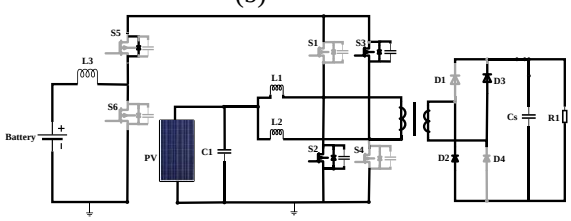

(c)

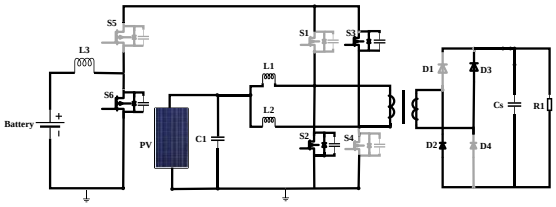

(d)

Figure 4. Equivalent operating circuits of mode 1 in time: (a) [t_0 - t_1), (b) [t_1 - t_2), (c) [t_2 - t_3), (d) [t_3 - t_4).

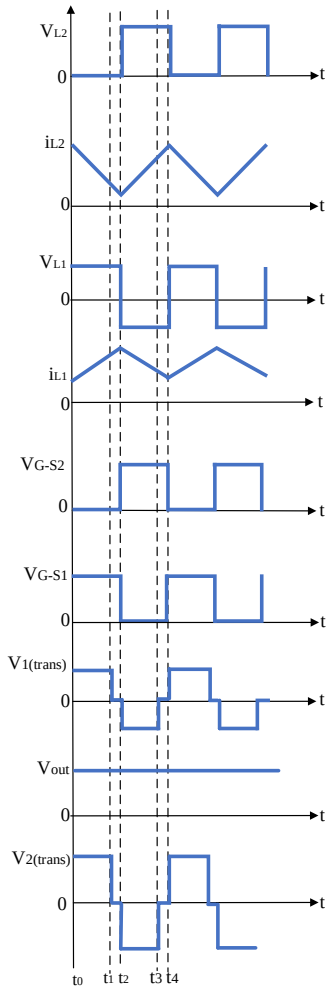

Figure 5. Waveform of the converter in mode 1.

Mode 2: In mode 2, due to the not available sunlight on the photovoltaic panel, its output power is zero, and in this mode, the battery charge is sufficient, and it is discharged. Mode 2 can be divided into 4 states, as briefly described in Table 1. The circuit in each of the operating modes is shown in Figure 6. The waveform of the converter in mode 2 is shown in Figure 7.

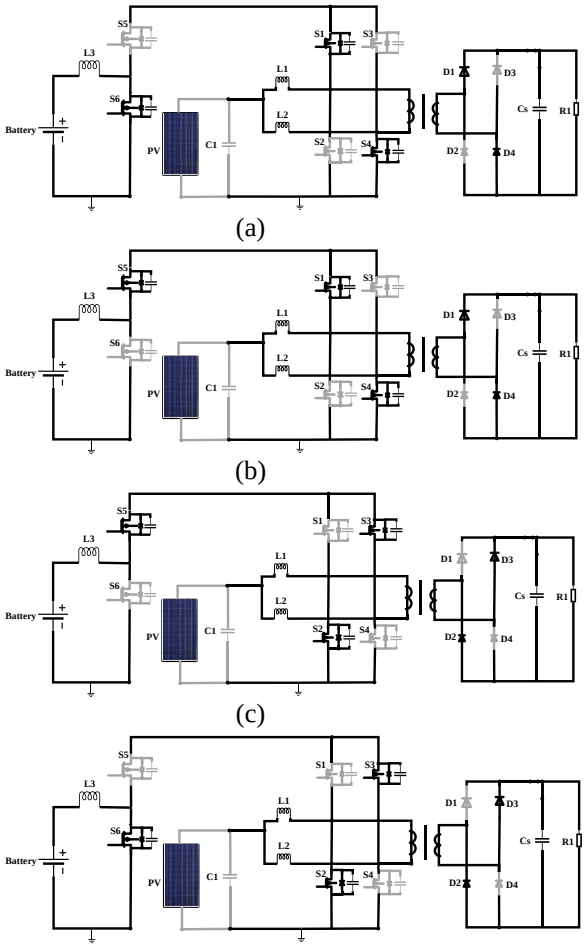

(a)

(b)

(c)

(d)

Figure 6. Equivalent operating circuits of mode 2 in time: (a) [t_0 - t_1), (b) [t_1 - t_2), (c) [t_2 - t_3), (d) [t_3 - t_4).

Mode 3: During this time, due to the sun's radiation, the photovoltaic panel produces power, and the load of the photovoltaic panel is available and is in MPPT mode. Also, in this mode, power is not received from the battery. As briefly explained in Table 1, this mode can be divided into 2 states. The circuit in each of the operating modes related to this mode is shown in Figure 8. The waveform of the converter in mode 3 is shown in Figure 9.

Mode 4: In this mode, the photovoltaic panel produces power, and the solar panel is in the MPPT mode. Also, in this case, the battery charge is insufficient, and the battery is charged. Mode 4 can be divided into 6 states, as briefly explained in Table 1. The circuit in each of the operating modes is shown in Figure 10. The waveform of the converter in mode 4 is shown in Figure 11.

As mentioned, in the proposed converter, the P&O algorithm is used to MPPT of the solar panel, and the PI control is used to control the output. The diagram of the system with its controllers is shown in Figure 12. d_1, d_2, d_3, and d_4 are the duty cycle for each switch.

According to the voltage balance law [26]:

$$DV_{pv} = (1-D)V_{bat} \tag{5}$$

According to the above, in this case, the secondary voltage of the transformer is determined as follows [26]:

$$V_2 = N(\frac{1-D}{D})V_{bat} + N(V_{bat}) = \frac{NV_{bat}}{D} \tag{6}$$

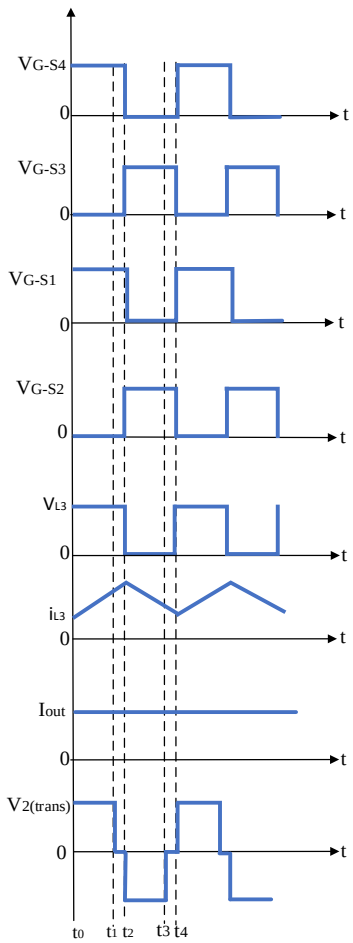

Figure 7. Waveform of the converter in mode 2.

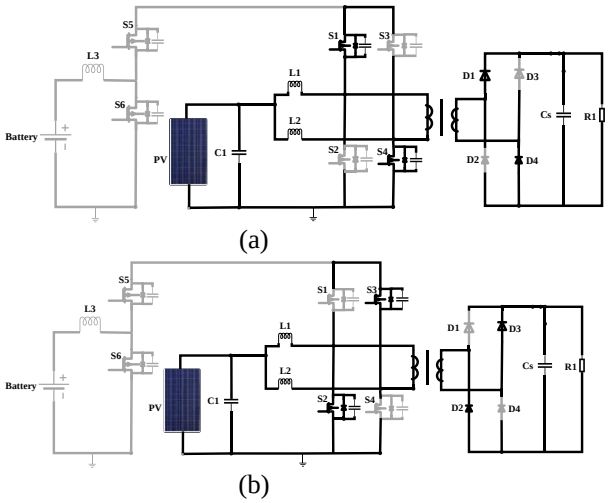

Figure 8. Equivalent operating circuits of mode 3 in time: (a) [t_0 - t_1), (b) [t_1 - t_2).

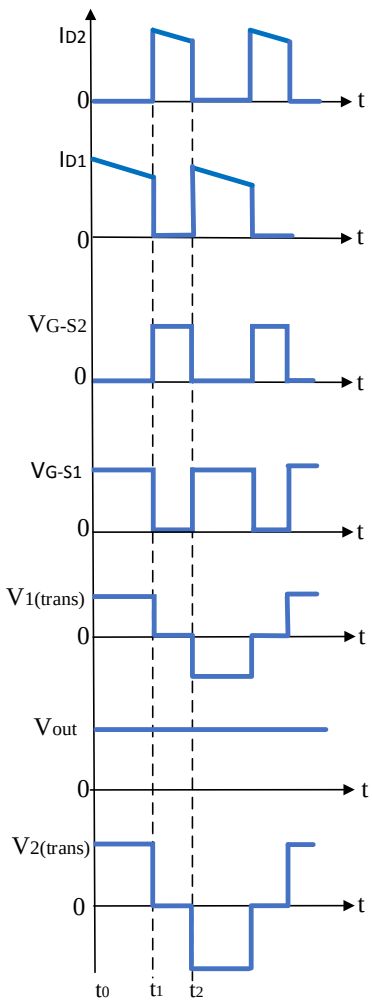

Figure 9. Some waveforms of the converter in mode 3.

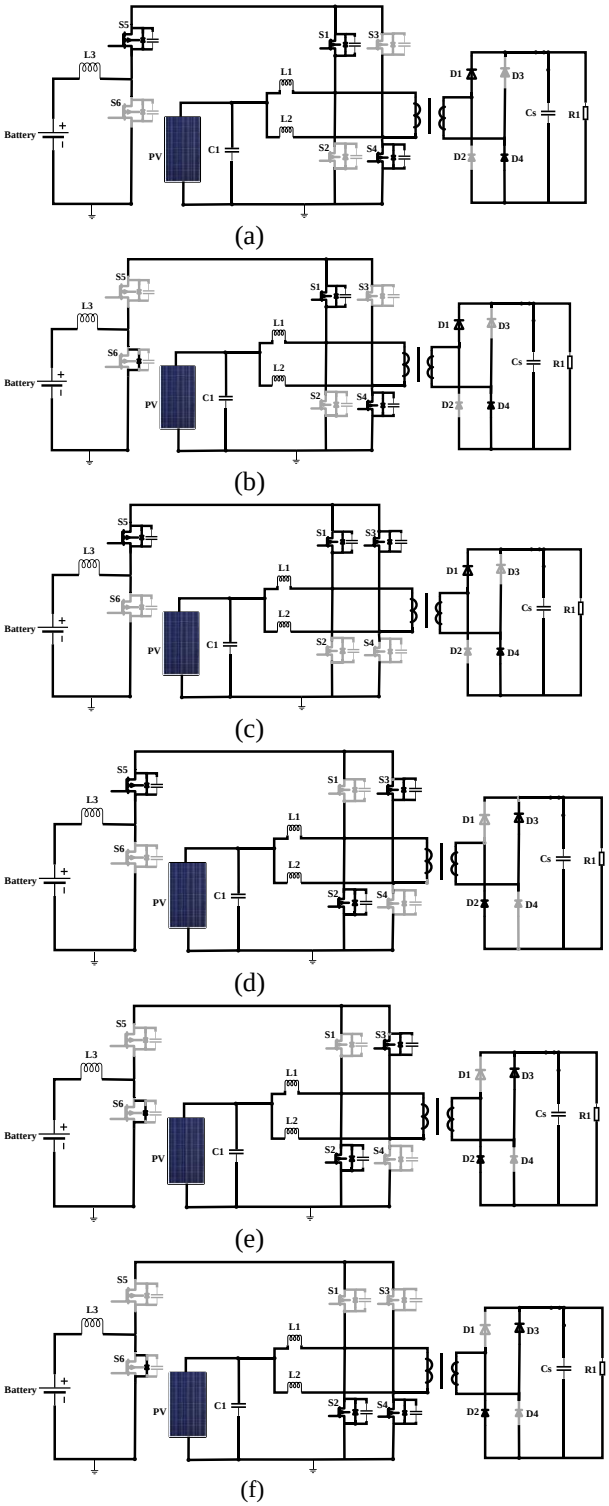

Figure 10. Equivalent operating circuits of mode 4 in time: (a) [t_0 - t_1), (b) [t_1 - t_2), (c) [t_2 - t_3), (d) [t_3 - t_4), (e) [t_4 - t_5), (f) [t_5 - t_6).

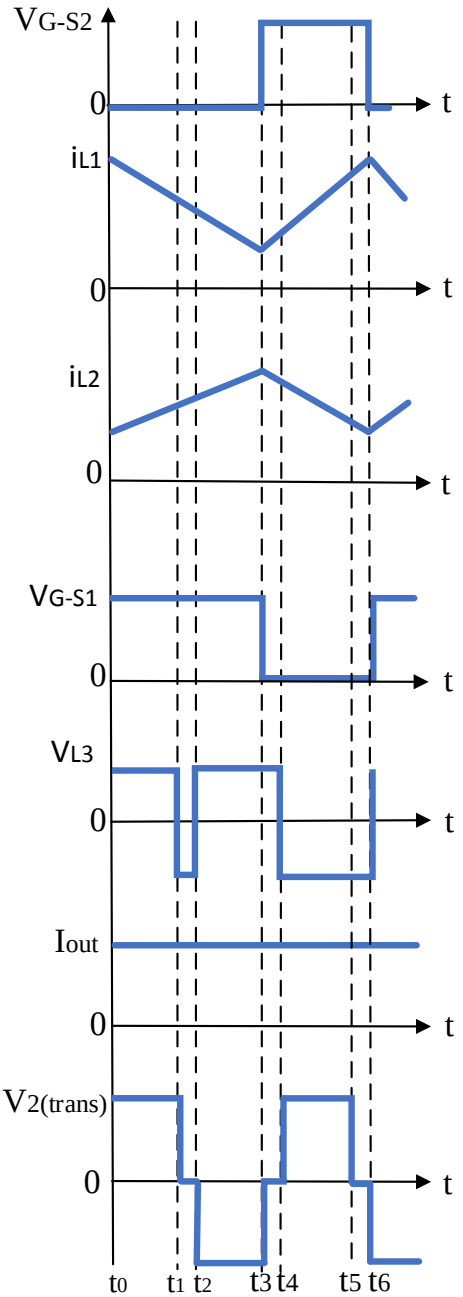

Figure 11. Waveforms of currents and inductors Voltages and gate-source voltage of MOSFETs in the proposed converter in mode 4.

Table 1. Performance of the converter

No. of mode	Conditions	time interval	State Numbers

1	S_2,S_3,Ds_5= off S_1, S_4, S_6 =on	[t_0-t_1)	1-1
	S_1,S_4, D_{S5} = on S_6, S_2, S_3 = off	[t_1-t_2)	1-2
	S_1, S_4, S_6 = off S_2, S_3,D_{S5} = on	[t_2-t_3)	1-3
	S_2, S_3, S_6 =on S_1,S_4,D_{S5}= off	[t_3-t_4)	1-4
2	S_2, S_3, S_5 = off S_1, S_4, S_6 = on	[t_0-t_1)	2-1
	S_1,S_6, S_4 = off S_2, S_3, S_5 = on	[t_1-t_2)	2-2
	S_2, S_3, S_6 = off S_1, S_4, S_5 =on	[t_2-t_3)	2-3
	S_1, S_4, S_5 =off S_2, S_3, S_6 = on	[t_3-t_4)	2-4
3	S_1, S_4, D_2, D_4 = on	[t_0-t_1)	3-1
	S_4, S_1 = off S_2, S_3 =on	[t_1-t_2)	3-2
4	D_2,D_3,S_3,S_2 ,S_6 = off D_1,D_4,S_5,S_4, S_1 = on	[t_0-t_1)	4-1
	D_2,D_3,S_5, S_3, S_2 = off D_1,D_4,D_{s5}, S_4, S_1 = on	[t_1-t_2)	4-2
	D_2,D_3,S_6,S_4, S_2 = off D_1,D_4,S_3,S_5, S_1 = on	[t_2-t_3)	4-3
	D_1,D_4,S_6,S_1, S_4 = off	[t_3-t_4)	4-4
	D_2,D_3,S_5,S_2, S_3 = on		
	D_1,D_4,S_5,S_1, S_4 = off D_2,D_3,D_{s6}, S_2, S_3 = on	[t_4-t_5)	4-5
	D_1,D_4,S_5,S_3, S_1 = off D_2,D_3,D_{s6},S_4, S_2 = on	[t_5-t_6)	4-6

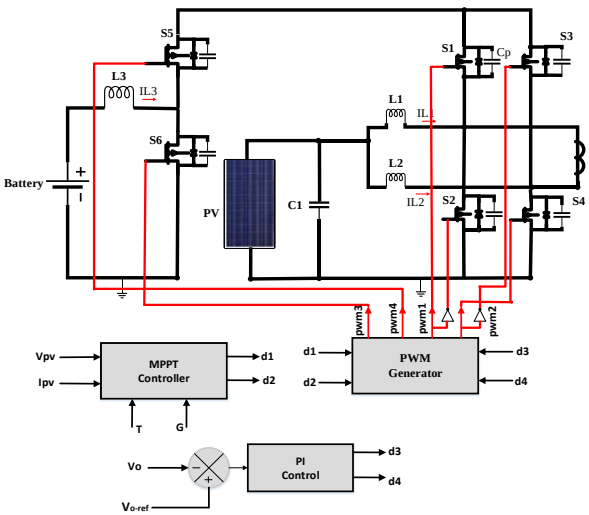

Figure 12. Block diagram of the system with the control section.

3. Design Considerations

In this section, the inductor and capacitor of the proposed converter are designed and discussed.

One of the design analyses of the converter is to calculate the current ripple and the input inductor [27], which is calculated according to the voltage of the battery, and the solar panel, which are the input voltages. The input current ripple is calculated according to the following equation [27]:

$$\Delta I_L = \frac{V_{out}}{2Lf_s} D(1-D) \quad (7)$$

The input inductance value of the converter is calculated as follows [27]:

$$L = \frac{V_{in}(V_{out} - V_{in})}{\Delta I_L f_s V_{out}} \quad (8)$$

Which is calculated according to the input current ripple in (7).

In all operating modes, the output capacitor Cs supplies the output load. The size of the output capacitor and the voltage ripple of the capacitor are calculated for mode 1. The voltage ripple of the output capacitor is calculated as follows [28]:

$$\Delta V_{cs}(t)=\frac{1}{c_s}(\int_{t0}^{t1} i_c(t)dt+\int_{t1}^{t2} i_c(t)dt+\int_{t2}^{t3} i_c(t)dt+\int_{t3}^{t4} i_c(t)dt) \quad (9)$$

The current of the output capacitor Cs (i_{cs}) is equal to the output current (i_{out}).

Output voltage ripples and output capacitor value with the help of the above relations are determined as follows [28]:

$$\Delta V_{out}=\frac{I_{out}D}{C_s f_s} \quad (10)$$

$$C_S=\frac{I_{out}D}{\Delta V_{out} f_s} \quad (11)$$

4. Simulation Results

The converter is simulated with MATLAB software to prove its efficiency. The parameters of the converter in the simulation are presented in Table 2. The proposed converter has two ports at the input. The first port is connected to a 120-watt solar panel, and the second port is connected to a 12-volt lithium-ion battery. The reference output voltage is considered to be 50 volts, and PI control is used to control the output of the converter. In this section, mode 1 is considered a study, and its results are stated.

The voltage waveform of the gate switches S_1, S_2, S_5, and S_6 is shown in Figure 13. It can be seen that during the period when switches S_1 and S_6 are on, switches S_2 and S_5 are off. The shape of the inductor currents L_1 and L_2 and the current of diodes D_1 and D_2 are shown in Figure 14. The output voltage is equal to 50 V and follows the value of the reference voltage. It can be seen that using a capacitor for the snubber circuit reduces overvoltage and fluctuations. The voltage, current, and output power waveforms are shown in Figure 15. The output power of the converter is equal to the designed value of 150 watts. The voltage waveform of the solar panel is shown in Figure 15(d), which is equal to the V_{max} of the solar panel at the MPPT point.

Table 2. Specifications of the converter proposed in the simulation

Parameter	Product/Value
L_1	150uH
L_2	150uH
L_3	220uH
Switches S_1-S_2-S_3-S_4-S_5-S_6	MOSFET N-Channel
C_S	4700uF
C_1	1000uF
$N = n_2 / n_1$	2
Voltage at P_{max} PV	24.1v
f_s	100KHz
Resistive load	15-70 (Ω)
V_{out}	50V

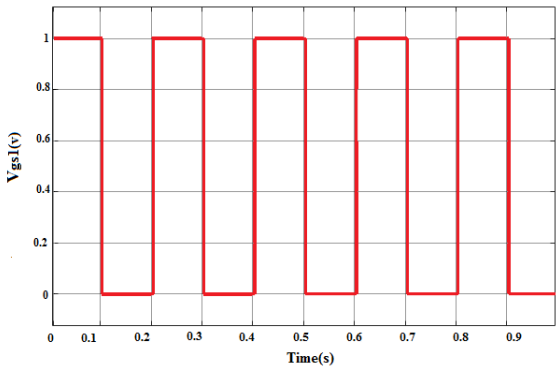

(a)

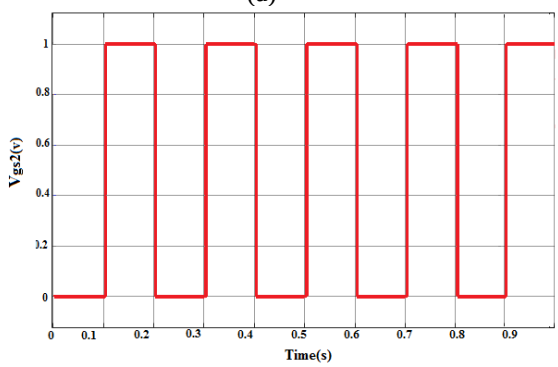

(b)

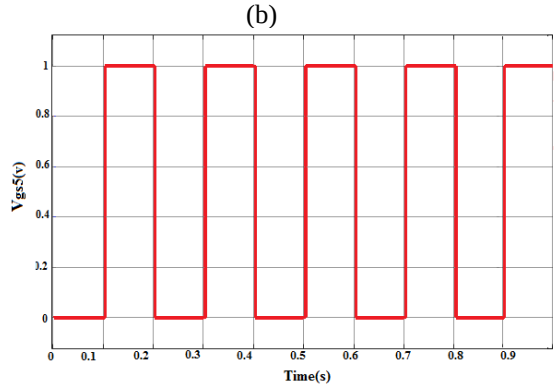

(c)

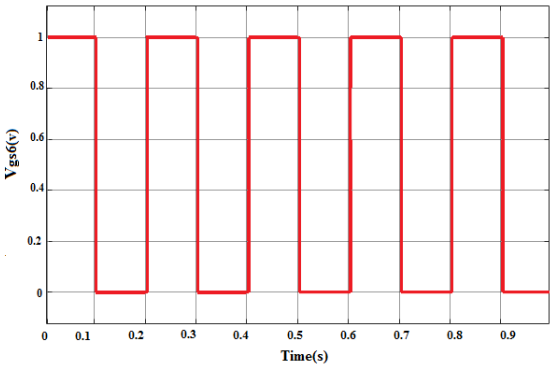

(d)

Figure 13. Gate voltage waveform of switches S_1, S_2, S_5, S_6 a) V_{gS1} b) V_{gS2} c) V_{gS5} d) V_{gS6}.

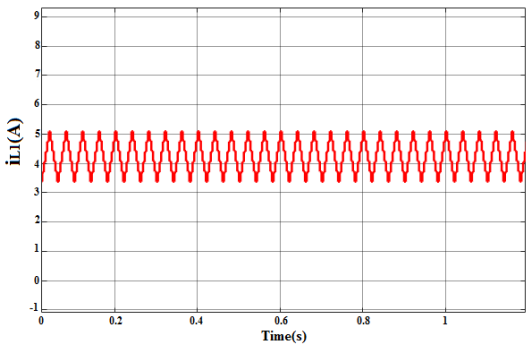

(a)

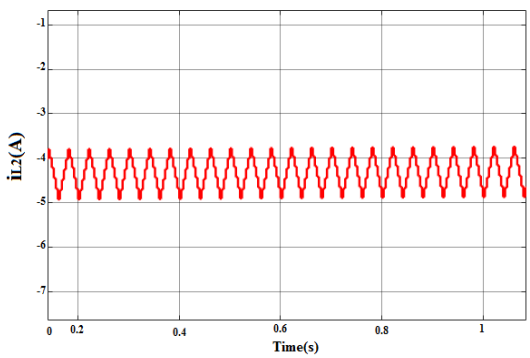

(b)

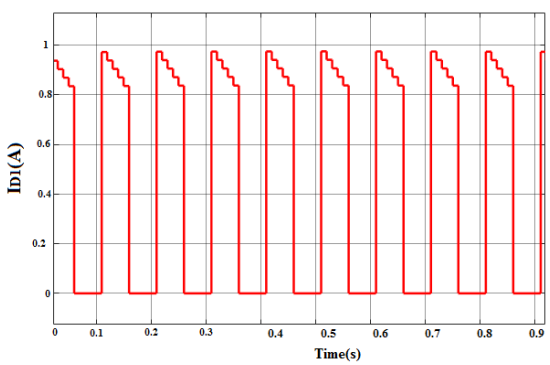

(c)

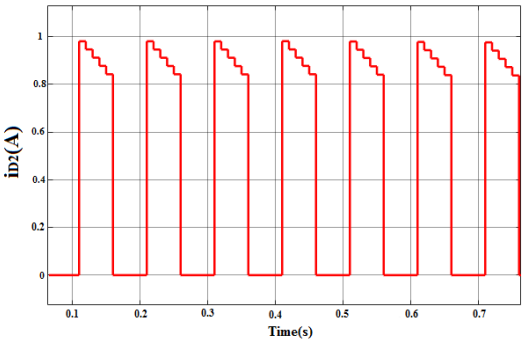

(d)

Figure 14. Current waveform D_1, D_2, L_2, L_1 a) I_{L1} b) I_{L2} c) I_{D1} d) I_{D2}.

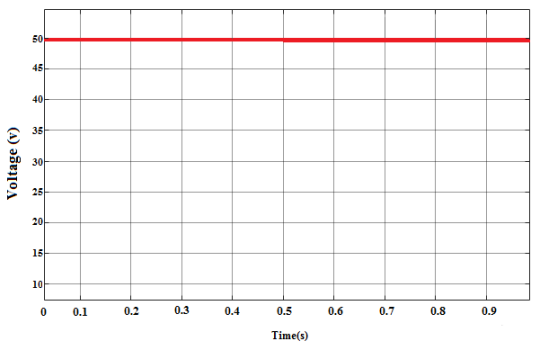

(a)

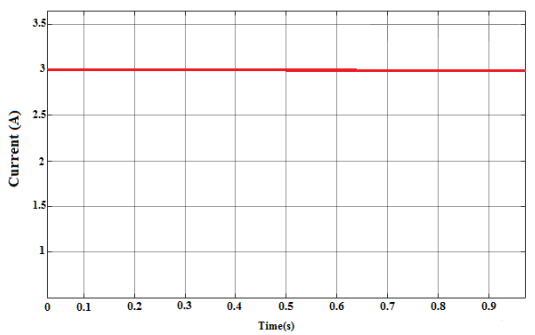

(b)

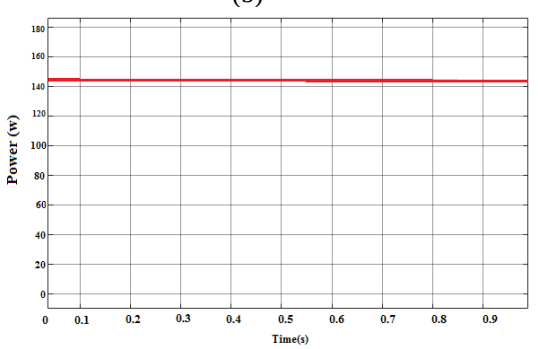

(c)

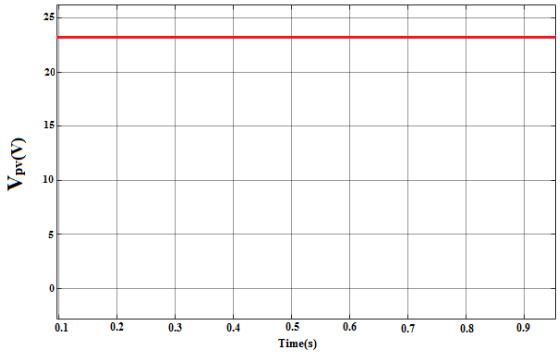

(d)

Figure 15. Simulation results of the converter a) V_{out} b) I_{out} c) P_{out} d) V_{pv}.

The simulation results confirm the performance of the proposed converter.

5. Performance comparison of the proposed converter

In choosing the required converter topology, the number of parts used in the converter and its efficiency have a great impact because these parameters can reduce the cost and improve the system performance; therefore, the proposed converter has been compared in terms of efficiency and the number of semiconductor parts (MOSFET-Diode) with four converters presented in the articles and the results are presented in Table 3.

Table 3. Comparison of the proposed converter and similar converters

Topology	No. of power switches (MOSFET + Diode)	Efficiency
Proposed	10	91%
[26]	9	90%
[29]	12	89%
[30]	9	76.1%
[31]	5	87%

6. Conclusions

In this paper, a three-port DC-DC converter is proposed for DC smart grid. In general, two converters are used to connect solar panels and batteries in the network, and the proposed structure with two inputs has increased efficiency and reduced the number of system elements. The first input is the solar panel converter, and the second input is the lithium-ion battery. The proposed converter is simulated at a power of 150 watts and a frequency of 100 kHz and has an efficiency of 91%. To improve the efficiency of the solar panel, the P&O algorithm has been used to MPPT in the simulation. The converter is simulated in MATLAB software, and the simulation results confirm the theoretical topics. The three-port converter is better in terms of the number of parts and cost than other topologies and has a more straightforward structure. The obtained results indicate the suitable performance of the converter for application in the DC smart grid. In this article, the new converter presented has a suitable performance and efficiency. To develop and continue working, more advanced methods can be used in the control part of the converter.

Acknowledgments

The authors would like to acknowledge the Imam Khomeini International University, Qazvin, Iran.

Nomenclature

C_s	output capacitor
DAB	dual active bridge
D	Duty cycle, value of D is limited between 0.5 and 1.
F_s	Switching frequency
HVS	High voltage side
I_{out}	output current of the converter
i_{cs}	current of the output capacitor Cs
$I_{min,s}$	minimum current values of Switch
LVS	Low voltage side
MPPT	Maximum Power Point Tracking
n	Ratio of primary to secondary turns of the transformer
N	The ratio of secondary to primary turns of the transformer
PV	Photovoltaic
P&O	Perturbation and observation
P_{pv}	Solar panel power
V_1	Primary voltage of the transformer(V)
V_2	Secondary voltage of the transformer(V)
V_{bat}	Battery voltage

V_{out}	Output voltage
V_{pv}	Solar panel voltage
V_{cs}	Capacitor voltage cs

References

[1] Z. W. Khan, H. Minxiao, C. Kai, L. Yang, and A. U. Rehman, (2020). "State of the Art DC-DC Converter Topologies for the Multi-Terminal DC Grid Applications: A Review," in 2020 IEEE International Conference on Power Electronics, Smart Grid and Renewable Energy (PESGRE2020), 1–7.

[2] H. Yang and M. Saeedifard, (2017). "A Capacitor Voltage Balancing Strategy With Minimized AC Circulating Current for the DC–DC Modular Multilevel Converter," IEEE Trans. Ind. Electron, 64(2), 956–965.

[3] G. P. Adam, I. A. Gowaid, S. J. Finney, D. Holliday, and B. W. Williams, (2016). "Review of dc–dc converters for multi- terminal HVDC transmission networks," IET Power Electron, 9(2), 281–296.

[4] L. Park, Y. Jang, S. Cho, and J. Kim, (2017). "Residential Demand Response for Renewable Energy Resources in Smart Grid Systems," IEEE Trans. Ind. Informatics, 13(6), 3165–3173.

[5] C. S. Lim and K. J. Lee, (2017). "Nonisolated two-phase bidirectional DC-DC converter with zero-voltage-transition for battery energy storage system," J. Electr. Eng. Technol, 12(6), 2237–2246.

[6] S. Liu, X. Liu, and Y.-F. Liu, (2015). "Analysis on feedback interconnections of cascaded DC-DC converter systems," in 2015 IEEE Energy Conversion Congress and Exposition (ECCE), 5160–5166.

[7] H. Li et al, (2022). "A Describing Function-Based Stability Analysis Method for Cascaded DC-DC Converters," IEEE Open J. Ind. Electron. Soc, 484–495.

[8] N. Mukherjee and D. Strickland, (2015). "Control of Cascaded DC-DC Converter Based Hybrid Battery Energy Storage Systems: Part – I: Stability Issue," IEEE Trans. Ind. Electron, 63(4), 1–4.

[9] B. Sri Revathi and M. Prabhakar, (2016). "Non isolated high gain DC-DC converter topologies for PV applications– A comprehensive review," Renew. Sustain. Energy Rev, 920–933.

[10] L. Schmitz, D. C. Martins, and R. F. Coelho, (2020). "Comprehensive Conception of High Step-Up DC–DC Converters With Coupled Inductor and Voltage Multipliers Techniques," IEEE Trans. Circuits Syst, 67(6), 2140–2151.

[11] Xiaofeng Zhang, Wei Chen, and Zhengyu Lu, (2008). "Key technologies of digital-current-controlled Bidirectional DC-DC converter in the hybrid electric vehicle," in 2008 IEEE Power Electronics Specialists Conference, 3104–3109.

[12] H. S. Lee and J. J. Yun, (2019). "High-Efficiency Bidirectional Buck-Boost Converter for Photovoltaic and Energy Storage Systems in a Smart Grid," IEEE Transactions on Power Electronics, 34(5), 4316–4328.

[13] R. Zhu, F. Hoffmann, N. Vazquez, K. Wang, and M. Liserre, (2020). "Asymmetrical Bidirectional DC–DC Converter With Limited Reverse Power Rating in Smart Transformer," IEEE Trans. Power Electron, 35(7), 6895–6905.

[14] B. S. Revathi and M. Prabhakar, (2022). "Solar PV Fed DC Microgrid: Applications, Converter Selection, Design and Testing," IEEE Access, 87227–87240.

[15] J. C. Rosas-Caro, F. Mancilla-David, J. C. Mayo-Maldonado, J. M. Gonzalez-Lopez, H. L. Torres-Espinosa, and J. E. Valdez-Resendiz, (2013). "A Transformer-less High-Gain Boost Converter With Input Current Ripple Cancelation at a Selectable Duty Cycle," IEEE Trans. Ind. Electron, 60(10), 4492–4499.

[16] P. K. Maroti, S. Padmanaban, J. B. Holm-Nielsen, M. Sagar Bhaskar, M. Meraj, and A. Iqbal, (2019). "A New Structure of High Voltage Gain SEPIC Converter for Renewable Energy Applications," IEEE Access, 89857–89868.

[17] R. A. Mastromauro, S. Pugliese, D. Ricchiuto, S. Stasi, and M. Liserre, (2015). "DC Multibus based on a Single-Star Bridge Cells Modular Multilevel Cascade Converter for DC smart grids," in 2015 International Conference on Clean Electrical Power (ICCEP), 55–60.

[18] R. Faraji, L. Ding, T. Rahimi, H. Farzanehfard, H. Hafezi, and M. Maghsoudi, (2021). "Efficient Multi-Port Bidirectional Converter With Soft-Switching Capability for Electric Vehicle Applications," IEEE Access, 107079–107094.

[19] S. Mukherjee, D. Mukherjee, and D. Kastha, (2019). "Multiport Soft-Switching Bidirectional DC-DC Converter for Hybrid Energy Storage Systems" in 2019 IEEE Applied Power Electronics Conference and Exposition (APEC), 2103–2109.

[20] M. Sarvi, S. Ahmadi, and S. Abdi. (2015). "A PSO-based maximum power point tracking for photovoltaic systems under environmental and

partially shaded conditions," Prog. Photovoltaics Res, 23(2), 201–214.
[21] M. a S. Masoum and M. Sarvi, (2005). "A new fuzzy-based maximum power point tracker for photovoltaic applications," Iran. J. Electr. Electron. Eng, 28–35.
[22] K. Nanshikar and A. Desai, (2016). "Simulation of P & O Algorithm using Boost Converter," IJIREEICE, 4(2), 130–135.
[23] M. Sarvi and A. Azadian, (2021). "A comprehensive review and classified comparison of MPPT algorithms in PV systems," Energy Syst, 13(2), 281-320.
[24] M. A. S. Masoum and M. Sarvi, (2008). "Voltage and current based MPPT of solar arrays under variable insolation and temperature conditions," in 2008 43rd International Universities Power Engineering Conference, 1–5.
[25]s A. A. de Melo Bento and E. R. Cabral da Silva, (2016). "Dual input single switch DC-DC converter for renewable energy applications," in 2016 12th IEEE International Conference on Industry Applications, 1–8.
[26] Y. Hu, W. Xiao, W. Cao, B. Ji, and D. J. Morrow, (2015). "Three-Port DC–DC Converter for Stand-Alone Photovoltaic Systems," IEEE Trans. Power Electron, 30(6), 3068–3076.
[27] T. Nouri, S. H. Hossein, E. Babaei, and J. Ebrahimi, (2016). "A non-isolated three-phase high step-up DC–DC converter suitable for renewable energy systems." Electric Power Systems Research, 140(16), 209-224.
[28] Ren L, Zhang L, Gong C, (2020). "ESR Estimation Schemes of Output Capacitor for Buck Converter from Capacitor Perspective." Journal of Electronics, 9(10), 1596-1608.
[29] P. Wang, P. Ren, X. Lu, W. Wang, and D. Xu, (2021). "Topology Analysis and Power Sharing Control of a Two-Stage Three-Port Hybrid Energy Storage Converter for DC Microgrids," IEEE Journal of Emerging and Selected Topics in Power Electronics, 9(1), 647–665.
[30] Z. N. Jan, (2021). "Microgrid: Innovation, Challenges and Prospects," Int. J. Res. Appl. Sci. Eng. Technol, 9(10), 484–489.
[31] P. Prabhakaran and V. Agarwal, (2020). "Novel Four-Port DC–DC Converter for Interfacing Solar PV–Fuel Cell Hybrid Sources with Low-Voltage Bipolar DC Microgrids," IEEE J. Emerg. Sel. Top. Power Electron, 8(2), 1330–1340.